ELSEVIER

Thin Solid Films 403–404 (2002) 252–257

thin solid films

www.elsevier.com/locate/tsf

Band energy diagram of CdTe thin film solar cells

J. Fritsche, D. Kraft, A. Thißen*, T. Mayer, A. Klein, W. Jaegermann

Surface Science Institute, Department of Materials Science, Darmstadt University of Technology, Petersenstraße 23, 64287 Darmstadt, Germany

Abstract

The knowledge of band energy diagrams of solar cells is essential for a fundamental understanding of their function. We have used photoelectron spectroscopy (PES) as a powerful tool for a systematic study of the formation of interfaces of CdTe solar cells in which the different layers CdS/SnO_2, CdTe/CdS and Te/CdTe are deposited step by step by thermal evaporation in model experiments. The results of these studies show that in contrast to other investigations the energy converting heterojunction is not a simple n-CdS/p-CdTe contact. Although depth profiling reveals a homogeneously intrinsic CdTe bulk layer, contact formation and $CdCl_2$-activation are assumed to form an n–i–p CdTe absorber. Such non-ideal conditions may strongly affect optimization processes of conversion efficiencies. The main limitations are evidently due to back-contact formation. Our results do not confirm that the electrochemically formed Te layer produces a good ohmic contact between the CdTe layer and the metallic back contact. From model experiments, we assume the formation of a tunneling contact, instead.

Keywords: Thin film solar cell; CdTe; CdS; Surface analysis; Photoemission; Band energy diagram

1. Introduction

The advantage of polycrystalline thin film solar cells like CdTe based cells compared to conventional devices is a reasonable conversion efficiency of approximately 10% and above reached by a low-cost production process. Fig. 1 shows the commonly used CdTe cell device structure as for example produced by ANTEC Solar GmbH using a close-space-sublimation (CSS) deposition process [2–5].

Effective improvement of the device structure is only possible based on a complete understanding of the device properties. Those properties are determined by structural influences [6–9] as well as by the electronic structure of the different interfaces resulting in the band energy diagram of the complete solar cell [10–12]. A powerful tool for studies of electronic structures of semiconductor surfaces and interfaces is photoelectron spectroscopy (PES) excited by X-rays (XPS) or by UV-light (UPS) [1]. But due to limited escape depths of the photoelectrons of approximately 10–50 Å the observation of inner interfaces of real devices is not possible. Therefore two complementary methods can be applied: (a) depth profiling at real devices by stepwise sputtering, etching or mechanical abrasion; or (b) gradual formation of the interfaces by adsorbate-on-substrate deposition as a model experiment for (a) accompanied by PES studies in both cases. Both types of studies were combined in this work in order to provide reliable data on the electronic interface structure.

2. Experimental

The XPS and UPS investigations were carried out using an integrated ultra-high vacuum (UHV) system that combines different in situ preparation techniques like molecular beam epitaxy (MBE) and sputtering in separated preparation chambers all connected to one transfer chamber with a high-resolution multitechnique surface science system Phi 5800 with monochromatized X-ray- and VUV-sources [7]. For MBE of metals and semiconductors, homemade Knudsen cells were used.

* Corresponding author. Tel.: +49-6151-166853; fax: +49-6151-166308.

E-mail address: athissen@surface.tu-darmstadt.de (A. Thißen).

0040-6090/02/$ - see front matter
PII: S0040-6090(01)01528-0

Fig. 1. Schematic cell device structure of a CdTe thin film solar cell.

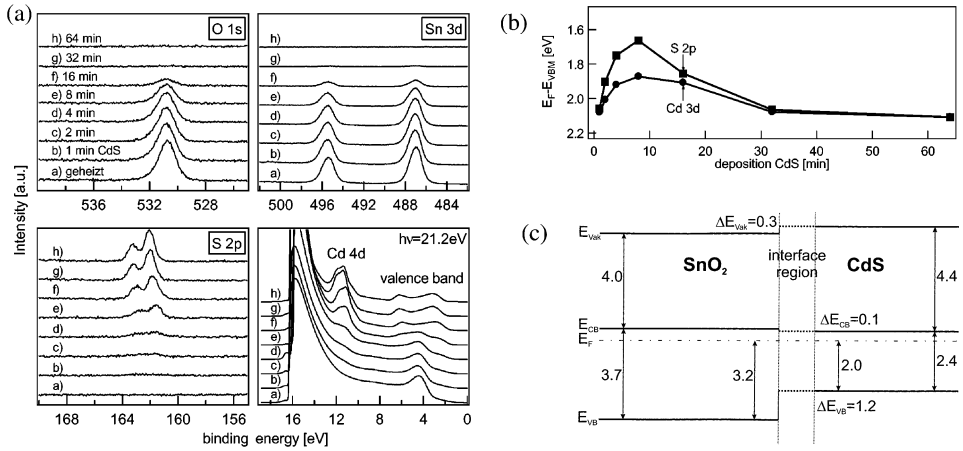

Fig. 2. (a) O1s-, Sn3d-, S2p-XP-spectra (AlKα) and VB-UP-spectra (HeI) of the SnO_2/CdS interface for different CdS deposition times corresponding to different CdS coverages. (b) Valence band (VB) position with respect to the Fermi-level for the SnO_2/CdS interface. (c) Band energy diagram of the SnO_2/CdS interface obtained by photoelectron spectroscopy.

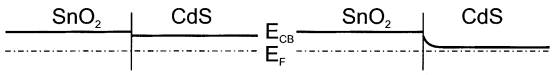

Fig. 3. Comparison of the conduction band alignment with low (left) and highly doped (right) CdS.

The evaporation rate was calibrated by a quartz microbalance. The overall energy resolution for AlKα excited photoelectron spectra is better than 400 meV and the base pressure of the system was below 10^{-9} mbar. The SXPS results were obtained at the undulator beamline U49/2 PGM2 at BESSY II. Surface morphologies after back contact etching were studied using an ex situ Thermomicroscopes CP AFM/STM, while step heights produced by depth profile etching have been controlled with a mechanical profilometer.

3. Results and discussion

Our results concerning the SnO_2/CdS- and the CdS/CdTe interface, the CdTe bulk doping and the CdTe/Te interface are summarized in this chapter. Finally, a band energy diagram for the whole device is proposed and discussed.

3.1. SnO_2/CdS interface

The transparent front contact of the CdTe solar cell consists of an indium tin oxide (ITO) layer of approximately 240 nm thickness on a glass substrate onto which

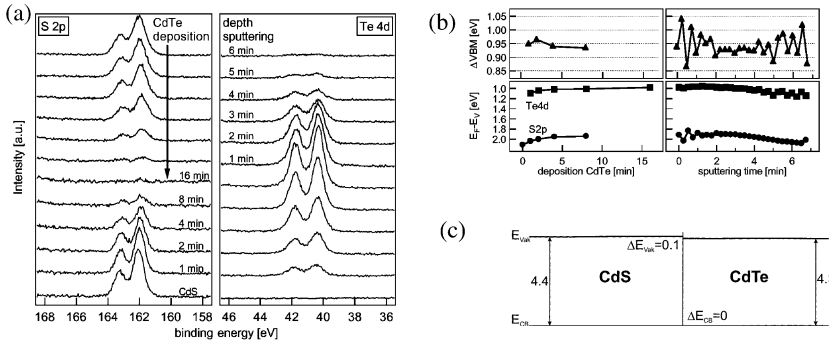

Fig. 4. (a) XP spectra of S2p and Te4d core levels for CdTe deposition and subsequent depth sputtering. (b) Valence band offsets and binding energies for the CdS/CdTe heterojunction. (c) Band energy diagram of the CdS/CdTe heterojunction.

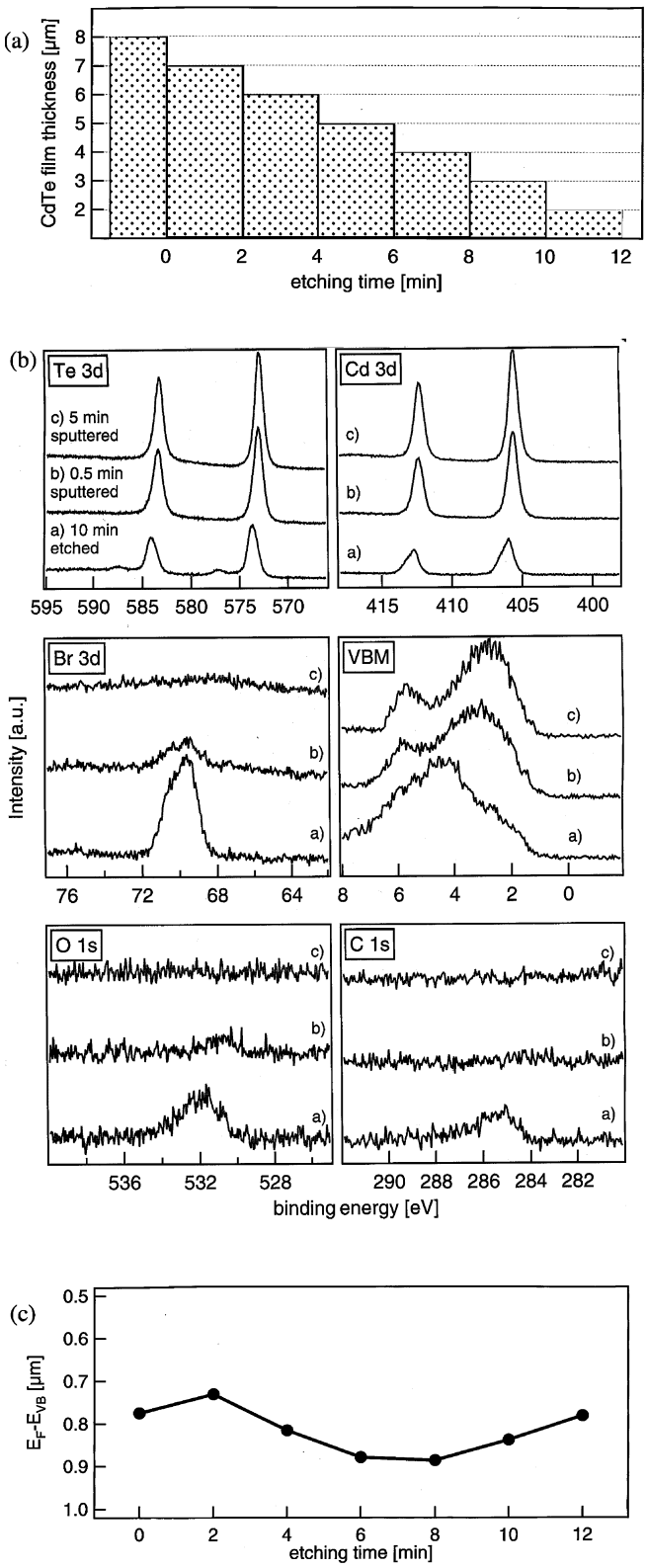

Fig. 5. (a) Remaining CdTe layer thicknesses after Br_2/methanol etch for different etching times. (b) XP spectra of a Br_2/methanol etched CdTe surface for different sputtering times. (c) Valence band position of CdTe for different etching times.

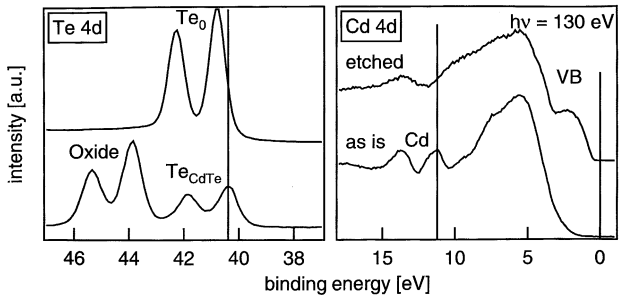

Fig. 6. SXP spectra of an untreated and an NP-etched CdTe layer.

a SnO_2 layer with 30 nm thickness is deposited. This SnO_2 layer is believed to act as a diffusion barrier for indium atoms. The SnO_2/CdS interface was gradually built up by deposition of thermally evaporated CdS onto a glass/ITO/SnO_2 substrate provided by ANTEC. XPS core level and UPS valence band spectra for different CdS deposition times and therefore CdS coverages are shown in Fig. 2a.

With increasing CdS coverage, the O1s- and Sn3d-substrate core level emissions disappear while the S2p-adsorbate emission appears. The valence band spectra change gradually from a SnO_2- to a CdS-type valence band. Binding energies were determined by a fit procedure. The binding energies of the core levels with respect to the binding energies of the valence band maximum are $BE_{VBM}(Cd3d) = 403.50$ eV and $BE_{VBM}(S2p) = 159.95$ eV. Therefore, the valence band positions with respect to the Fermi-level can be calculated. These are shown in Fig. 2b. For deposition times below 30 min, the calculated VB positions from S2p and Cd3d are different. At higher deposition times, the values converge again. That means that for low coverages no bulk-like CdS layer is formed due to interdiffusion or stress and strain at the interface. The resulting band energy diagram is shown in Fig. 2c. The valence band offset is 1.2 eV and the conduction band offset is approximately 0.1 eV. The difference of the conduction band minimum with respect to the Fermi level is 0.4 eV. Hence, 0.4 eV would occur as a loss in the photovoltage of the solar cell. This is not observed by electrical measurements. This photovoltage reduction can only be avoided by a strong band bending caused by a highly n-doped CdS. This situation is shown in Fig. 3.

In a recent publication [13] it is shown that annealing in $ZnCl_2$ can change the CdS to a highly n-doped

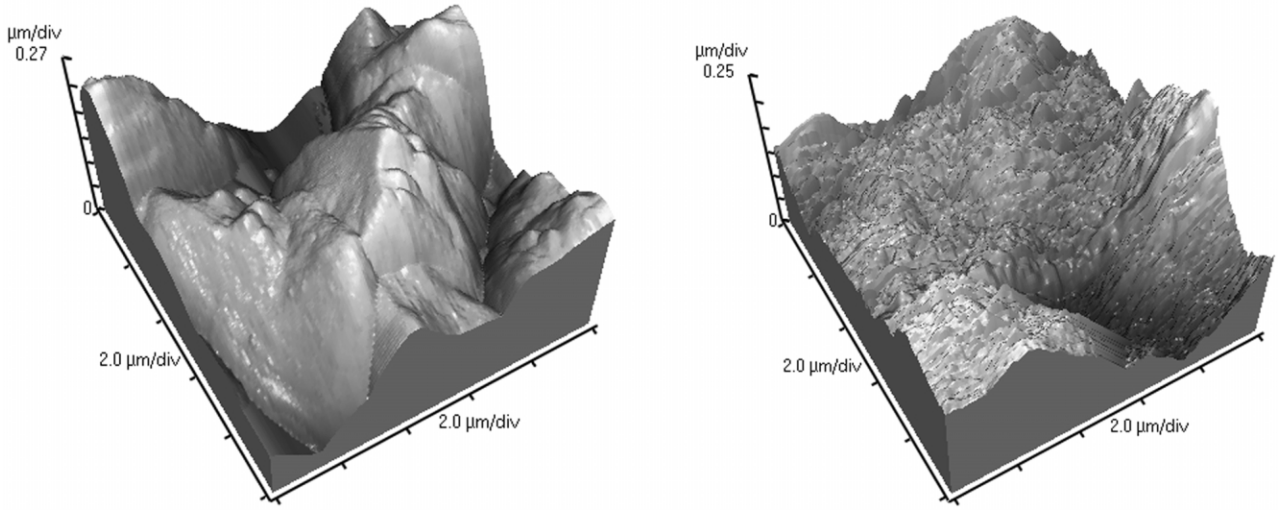

Fig. 7. AFM topography of an untreated (left) and an NP-etched CdTe layer (right).

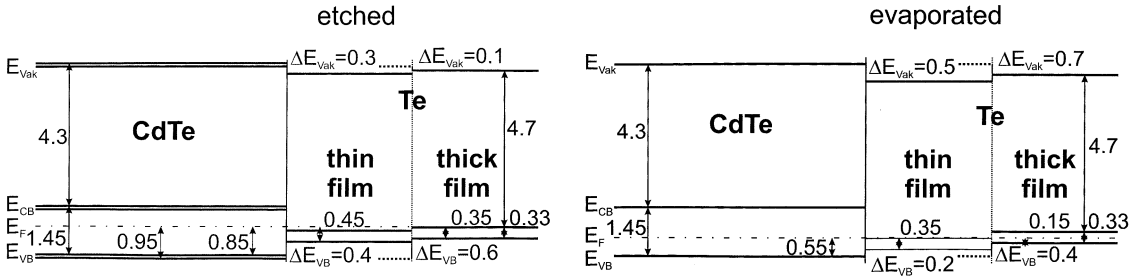

Fig. 8. Comparison of the band energy diagram of Te/CdTe formed by etching and by evaporation.

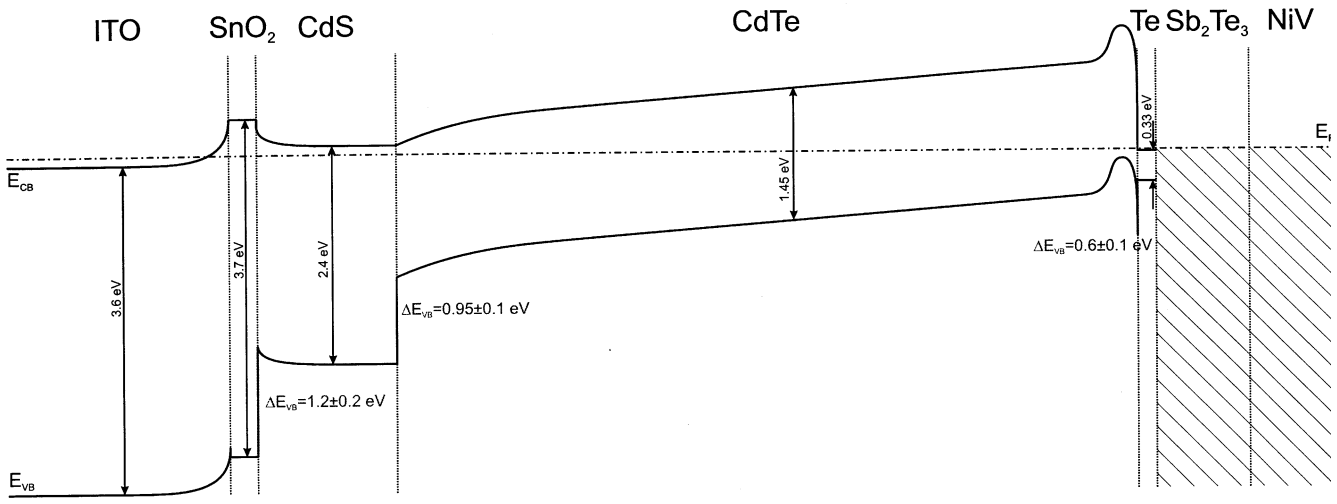

Fig. 9. Proposed band energy diagram of the CdTe thin film solar cell.

material with electron concentrations up to 10^{20} cm^{-3}. From this, it can be assumed that one effect of the $CdCl_2$ activation step of the CdTe solar cell [9] is strong n-doping of the CdS. The only disadvantage of a highly n-doped CdS would be a serial resistance due to the SnO_2 conduction band position. Further investigations of the CdS doping by $CdCl_2$ have to be carried out in order to prove this assumption.

3.2. CdS/CdTe interface

The CdS/CdTe interface forms the heterocontact of the CdTe thin film solar cell. As substrate for the CdTe deposition, a glass/ITO/SnO_2/CdS sample (see Section 3.1) is used. The CdTe is deposited by thermal evaporation on to this substrate and afterwards the CdTe film is gradually removed by depth profile sputtering. Photoelectron spectra are shown in Fig. 4a. The S2p line intensity decreases and the Te4d line intensity increases with increasing CdTe layer thickness. The binding energies of the valence band maximum and the valence band offsets shown in Fig. 4b are calculated from the core level binding energies of Fig. 4a using $BE_{VBM}(S2p) = 195.97$ eV and $BE_{VBM}(Te4d) = 39.35$ eV. The resulting band energy diagram for the heterojunction is shown in Fig. 4c. The valence band offset is 0.95 eV and there is no conduction band offset. The thermally evaporated CdTe is slightly n-doped with $E_F - E_{VB} =$ 1.05 eV.

3.3. CdTe bulk doping

The doping of the CdTe layer is important information for the understanding of the CdTe solar cell device. Therefore a depth profile produced by etching with 0.5% Br_2/methanol of a complete ANTEC cell without back contact has been studied with photoelectron spectroscopy. In Fig. 5a the remaining CdTe layer thicknesses for different etching times are shown.

After etching, the surface shows O, C and Br contamination (Fig. 5b). They can completely be removed by mild sputtering for 5 min. The valence band positions with respect to the Fermi level can be derived from these spectra. These are shown in Fig. 5c. The data show only a slight variation of approximately 0.10 eV along the CdTe layer which is therefore more or less homogeneously intrinsic. This result suggests that in contrast to earlier studies [5] the energy converting region of the CdTe thin film solar cell is not a simple n-CdS/p-CdTe heterojunction.

3.4. CdTe/Te interface

Formation of ohmic back contacts on CdTe needs chemically inactive high work function materials. The optimal material has not yet been found. The common back contact consists of an elemental Te layer formed by etching with NP-etch (60% H_3PO_4, 1% HNO_3, 39% H_2O) [14–18]. The back contact materials Sb_2Te_3 and NiV are deposited on to that layer. In Fig. 6 the effect of the etching process on the CdTe layer is shown. The surface oxide is removed from the surface and the Te layer is formed by dissolution of Cd from the sample.

Atomic force microscopy (AFM) topography (Fig. 7) shows a micro-roughening of the surface due to preferential etching along grain boundaries.

The left graph in Fig. 8 shows the resulting band energy diagram for a thick and a thin Te layer on CdTe formed by etching. For a thick Te layer, the valence band offset is 0.60 eV and the valence band position for CdTe is 0.95 eV. For a thin layer, the valence band offset decreases to 0.40 eV and CdTe valence band position decreases by 0.10 eV. The valence band offsets show that the Te layer does not form a good ohmic

contact on CdTe. The Te thickness dependence of the valence band positions of CdTe indicates a change in the doping due to back contact formation. For comparison, an elemental Te layer has been deposited on a CdTe layer by thermal evaporation. The results of this experiment are shown in the right graph of Fig. 8. The latter procedure leads to smaller valence band offsets and to a CdTe valence band position that is independent of Te film thickness. In contrast to etched CdTe layers, a deposited Te layer does not lead to reasonable conversion efficiencies of the cell [15]. Therefore, it is suggested that a Te layer formed by etching leads to a tunneling contact to CdTe if this is strongly p-doped. This assumption is in good agreement with electrical measurements [19,20].

4. Conclusion

The complete band energy diagram in Fig. 9 summarizes the results of this work when combined with two assumptions that have to be proven in our next experiments.

The first assumption is the strong n-doping of the CdS by the $CdCl_2$ treatment. The second assumption is the strong p-doping of the CdTe at the Te/CdTe interface at the back contact leading to a tunneling contact. These assumptions convert the intrinsic CdTe layer into an n–i–p–CdTe structure that would be in good agreement with the results of electrical measurements [19,20].

Acknowledgements

The authors would like to thank ANTEC Technology GmbH for the collaboration and the group of Prof. Dr D. Schmeisser from the BTU Cottbus for their equipment used at BESSY II. This work was supported by the Bundesministerium für Wirtschaft (BMWi) Grant No. 0329857.

References

[1] W. Mönch, Semiconductor Surfaces and Interfaces, Springer, Berlin, 2001.
[2] T.L. Chu, Curr. Topics Photovolt. 3 (1988) 235.
[3] K. Zweibel, R. Mitchell, Adv. Solar Energy 6 (1991) 485.
[4] W.H. Bloss, F. Pfisterer, M. Schubert, T. Walter, Prog. Photovolt. Res. Appl. 3 (1995) 11.
[5] D. Bonnet, M. Harr, Proc. 2nd Int. Conf. Photovolt. Solar Energy Conv. 1 (1998) 397.
[6] J. Fritsche, S. Gunst, E. Golusda, M.C. Lejard, A. Thißen, T. Mayer, A. Klein, R. Wendt, R. Gegenwart, D. Bonnet, W. Jaegermann, Thin Solid Films 387 (2001) 161.
[7] J. Fritsche, D. Kraft, A. Thißen, T. Mayer, A. Klein, W. Jaegermann, MRS Prc. (2001) (in press).
[8] M.A. Cousins, K. Durose, Thin Solid Films 361/362 (2000) 253.
[9] H. Moutinho, M. Al-Jassim, D. Levi, P. Dippo, L. Kazmerski, J. Vac. Sci. Technol. A16 (1998) 1251.
[10] J. Fritsche, A. Thißen, A. Klein, W. Jaegermann, Thin Solid Films 387 (2001) 158.
[11] J. Fritsche, S. Gunst, A. Thißen, R. Gegenwart, A. Klein, W. Jaegermann, MRS Prc. (2001) (in press).
[12] D. Kraft, A. Thißen, M. Campo, T. Mayer, A. Klein, W. Jaegermann, MRS Prc. (2001) (in press).
[13] M. Grün, A. Storzum, M. Hetterich, A. Kamilli, W. Send, T. Walter, C. Klingshirn, J. Crystal Growth 201/202 (1999) 457.
[14] J. Sarlund, M. Ritala, M. Leskelä, E. Siponmaa, R. Zilliacus, Sol. En. Mater. Sol. Cells 44 (1996) 177.
[15] D. Niles, X. Li, P. Sheldon, H. Höchst, J. Appl. Phys. 77 (1995) 4489.
[16] X. Li, D. Niles, F.S. Hasoon, R.J. Matson, P. Sheldon, J. Vac. Sci. Technol. A17 (1999) 805.
[17] D. Bätzner, R. Wendt, A. Romeo, H. Zogg, A.N. Tiwari, Thin Solid Films 361/2 (2000) 463.
[18] D. Bätzner, A. Romeo, H. Zogg, R. Wendt, A.N. Tiwari, Thin Solid Films 387 (2001) 151.
[19] G. Stollwerck, J.R. Sites, Proc. of the 13th Europ. Photovolt. Sol. En. Conf. Nice, 1995, p. 2020.
[20] T.J. McMahon, A.L. Fahrenbruch, Proc. of the 28th IEEE PVSC Anchorage, Alaska, 2000.